Structural and spectroscopic investigation of new luminescent hybrid materials based on calix[4]arene-tetracarboxylate and Ln^{3+} ions (Ln = Gd, Tb or Eu)

R.S. Viana[a], C.A.F. Oliveira[a,b], J. Chojnacki[c], B.S. Barros[d], S. Alves-Jr[a], J. Kulesza[a,*]

[a] Department of Fundamental Chemistry, Federal University of Pernambuco, Av. Prof. Moraes Rego, 1235 - Cidade Universitária, 50670-901 Recife, PE, Brazil
[b] Federal Institute of Paraiba (IFPB), Av. Primeiro de Maio, 720-Jaguaribe, 58015-435 João Pessoa, PB, Brazil
[c] Department of Inorganic Chemistry, Chemical Faculty, Gdansk University of Technology, G. Narutowicza 11/12 Street, 80-233 Gdansk, Poland
[d] Department of Mechanical Engineering, Federal University of Pernambuco, Av. Prof. Moraes Rego, 1235 - Cidade Universitária, 50670-901 Recife, PE, Brazil

ARTICLE INFO

ABSTRACT

Lanthanide-calixarene hybrid materials are of particular interest due to the combination of the interesting properties of the ligand cavity-like structure and the luminescent features of lanthanides. The aim of this study was to synthesize and investigate the photophysical properties of Eu^{3+}, Tb^{3+} and Gd^{3+} hybrids based on calix[4]arene-tetracarboxylate. The preparation of two structurally different Tb^{3+} compounds (calix-TA-SC-Tb and calix-TA-Tb) was dictated by the ligand to metal molar ratio and the synthesis time. Analysis of calix-TA-SC-Tb monocrystals revealed the formation of a mononuclear complex of C$_2$ symmetry containing Tb^{3+} coordinated by four calixarene ionized groups and formate anion encapsulated within the upper cavity. Syntheses of other hybrids failed in producing high-quality crystals and the structures could not be solved. The solid-state luminescent properties of hybrids were evaluated, and the structure/property relationship was investigated. Based on the emission and excitation spectra, the energy diagrams for calix-TA-Eu, calix-TA-Tb and calix-TA-Gd were proposed.

1. Introduction

Calixarenes represent a class of macrocyclic ligands commonly used for the preparation of diverse self-assembled supramolecular structures, including organic-inorganic hybrid materials [1,2]. When functionalized, these macrocycles are capable of interacting with various metal ions forming stable inclusion complexes of the host-guest type [3]. More recently, modified calixarenes have successfully been used as secondary building units to prepare extended structures, coordination polymers [4]. The use of calixarenes for the construction of hybrid materials is particularly interesting due to the unique properties of these ligands, such as a tunable cavity, conformational flexibility, and diversity of the structure modification [1]. All these features potentially favor the formation of extended intriguing structures. Currently, the construction of coordination polymers based on calixarenes has mainly been focused on upper-rim functionalized calixarenes such as calixarene-sulfonates [5–7]. Only a few papers have been reported on coordination polymers based on calixarenes appended with polycar-

boxylate groups on the upper [8,9] or the lower rim [10,11].

Among versatile hybrid materials based on calixarenes, those containing lanthanide ions are of particular interest due to the intrinsic properties of lanthanide ions combined with the unique properties of macrocyclic compounds. Although, the preparation of lanthanide-hybrid materials based on calixarenes have been reported [9,12,13], little has been revealed on the luminescent properties of such materials, especially those of extended structures.

This paper presents the synthesis and photophysical properties of hybrid materials based on p-tert-butylcalix[4]arene tetracarboxylic acid (calix-TA) and lanthanide ions (Eu^{3+}, Tb^{3+} or Gd^{3+}). The obtained products were characterized by XRD, IR spectroscopy and photoluminescent solid-state spectroscopy.

* Corresponding author.
E-mail address: joanna.kulesza@ufpe.br (J. Kulesza).

2. Experimental

2.1. Material and Methods

The ligand *p-tert*-butyl-25,26,27,28-tetrakis(carboxymethoxy)calix[4]arene (calix-TA), was prepared according to the procedure reported in [14,15] starting from *p-tert*-butylcalix[4]arene purchased from Alfa Aesar.

Europium, terbium and gadolinium oxides were purchased from Sigma-Aldrich and were used as received to prepare the corresponding lanthanide chlorides by treatment with concentrated hydrochloric acid (HCl). Solvents; dimethylformamide (DMF) and acetonitrile (ACN) were acquired from Vetec and were used as received without further purification.

Single-crystal X-ray diffraction data were collected on a KUMA KM4CCD κ-axis diffractometer with graphite monochromated Mo Kα radiation (λ=0.71073 Å) at 298 K. The collected data were processed using the CrysAlisPro (Agilent Technologies) program package [16]. Empirical absorption correction (multi-scan) was applied using spherical harmonics, implemented in SCALE3 ABSPACK scaling algorithm of the CrysAlisPro package. An initial structure model was obtained by charge flipping (SUPERFLIP, Palatinus) [17]. Calculations were carried out using the SHELX system [18] run under WINGX environment [19]. Visualization and analysis of crystal structure were performed using the Mercury program [20].

Powder X-ray diffraction (PXRD) data were recorded at room temperature on a Siemens diffractometer model D5000 with Cu Kα (λ=1.5406 Å) radiation. Fourier Transform Infrared spectra (FT-IR) were measured on a Bruker spectrometer (model IFS66) at the range of 4000−400 cm^{-1} using KBr pellets. The photoluminescence properties were investigated using a spectrofluorometer Horiba-Jobin Yvon Fluorolog-3 with a continuous 450 W xenon lamp and UV xenon flash tube for excitation, double-grating monochromator in the excitation and UV−vis (ultraviolet-visible) emission position, single-grating monochromator in the NIR (near infrared) emission position, R928P and H10330A-75 Hamamatsu photomultipliers respectively to UV−vis range emissions. All emission spectra were corrected for the wavelength dependent response of the detection system. A silicon photodiode reference detector was used to monitor and compensate the variation in the xenon lamp output, using typical correction spectra provided by the manufacturer. Measurements of luminescence lifetimes were performed on the same spectroscopic apparatus but with a 450 W xenon lamp in a pulse mode.

The emission quantum efficiency (η) was calculated according to the Eq. (1), where A_{rad} is the radiative decay rate obtained by summing over the radiative rates $A_{0,J}$ for each $^5D_0 \rightarrow {}^7F_J$ (J=0−4) transitions. The total radiative decay rate (A_{total}) is given by the relation $A_{total}=\tau^{-1}$, where τ is the lifetime for the radiative decay associated with the $^5D_0 \rightarrow {}^7F_2$ transition. Finally, the non-radiative decay rate (A_{nrad}) is given by the difference $A_{nrad}=A_{total} - A_{rad}$ [21,22].

$$\eta = \frac{A_{rad}}{A_{rad} + A_{nrad}} x100\% \qquad (1)$$

2.2. Synthesis

The synthesis of calix-tetracarboxylate hybrid materials was performed using the slightly modified procedure described in [9].

2.2.1. Synthesis of calix-TA-Ln (Ln = Eu, Tb or Gd)

A DMF solution (6 mL) of the ligand calix-TA (53 mg, 0.06 mmol) was added to a beaker containing an ACN solution (6 mL) of the respective lanthanide chloride (0.02 mmol), and the mixture was placed in a thick-walled glass tube which was subsequently transferred to an oven. The reaction was carried out at 90 ºC for four days. After that time, the resulting powders of calix-TA-Eu, calix-TA-Tb or calix-

TA-Gd (insoluble in water or any organic solvent) were filtered off, washed with DMF and dried in an oven at 60 ºC for 2 h.

2.2.2. Synthesis of calix-TA-SC-Tb

The single complex of calix-TA and Tb^{3+} was prepared as follows: a DMF solution (6 mL) of calix-TA (53 mg, 0.06 mmol) was added to a beaker containing an ACN solution (6 mL) of terbium chloride (0.06 mmol) and then pH of the solution was adjusted to 1 with 1 M HCl. The mixture was placed in a thick-walled glass tube which was subsequently transferred to an oven. The reaction was carried out at 90 ºC for 24 h. After that time, the mixture was slowly cooled down to room temperature. Colorless crystals as cubic blocks were isolated, collected by filtration, washed with DMF and dried at 60 ºC for 2 h. For single-crystal X-ray diffraction measurements, crystals of calix-TA-SC-Tb were taken directly from the mother liquid solution without drying.

3. Results and discussion

3.1. Synthesis

Two different self-assembled structures calix-TA-Tb and calix-TA-SC-Tb were obtained by varying the ligand to metal ratio from 3:1 to 1:1, respectively. In the synthesis of other two hybrid materials calix-TA-Eu and calix-TA-Gd, the L/M molar ratio was maintained at 3:1. In the case of calix-TA-SC-Tb, one day was sufficient to produce good-quality crystals suitable for single-crystal X-ray analysis. Formation of other materials required four days and always failed to form single crystals. Therefore, for calix-TA-Ln, only powder X-ray diffraction experiments were conducted.

3.2. Structure description

Crystal data, data collection and structure refinement for calix-TA-SC-Tb are summarized in Table 1. Further details of the structure refinement for calix-TA-SC-Tb can be found in Supporting information (Tables S1-S3).

Compound calix-TA-SC-Tb crystallizes in the triclinic system in the space group P$\bar{1}$. Structure is composed of a molecular, mononuclear anionic complex containing terbium cation coordinated by ionized calixarene and a formate anion (HCOO$^-$), surrounded by a dimethylamonium cation (Me$_2$NH$_2{}^+$), the hydronium cation (H$_2$O-H-OH$_2{}^+$) and three solvating water molecules in the second coordination sphere. The formate anions and dimethylammonium cations may originate from the hydrolysis of DMF. The asymmetric unit is shown in Fig. 1.

Due to the charge balance, one of the free oxygen atoms has to be regarded as an H$_3$O$^+$ cation. We have five negative charges: calix-carboxylate (four groups)+formate. On the positive side, we have Tb^{3+} and (Me$_2$NH$_2{}^+$) which leaves one positive charge to be placed on oxygen (if we exclude the possibility of Tb^{4+} formation). Location of the hydrogen atoms is not certain based on the diffraction data. Nevertheless, e.g. separation of O18 and O19 is only 2.418 Å, which is typical for the hydronium cation (also called Zundel ion) [23,24] containing charge-assisted hydrogen bonding [H$_2$O...H...OH$_2$]$^+$. One of the water molecules (O16) forms hydrogen bonding with the formate ion; the other molecules are attached by hydrogen bonding to oxygen atoms. The terbium cation has a coordination number of nine, with the coordination polyhedron being distorted capped tetragonal antiprism. Oxygen donor atoms from the calix residue form the tetragonal antiprism, while the ninth oxygen donor atom is located above the upper square of the antiprism. The overall symmetry of coordination environment can be approximated by Schoenflies C$_2$ group. The formate ligand has the shortest Tb—O bond (2.364(3) Å) and is located inside the calixarene cavity. Mean bond length for the etheric O—Tb bonds is 2.492, while for carboxylic O—Tb bonds is 2.390 Å. The shortest distance between two terbium atoms is 9.064 Å (between Tb1 and its equivalent generated by inversion about (½,0,0), which is less

Table 1
Crystal data, data collection and structure refinement for calix-TA-SC-Tb.

Crystal data	
Chemical formula	$C_{53}H_{61}O_{14}Tb \cdot C_2H_8N \cdot O_2H_5 \cdot 3(OH_2)$
Formula weight	1207.03
Crystal system, space group	Triclinic, $P\bar{1}$
Temperature (K)	298
a, b, c (Å)	11.3359 (4), 12.6499 (4), 22.9920 (9)
α, β, γ (°)	86.976 (3), 83.813 (3), 69.051 (3)
V (Å³)	3060.78 (19)
Z	2
Radiation type	Mo $K\alpha$, λ=0.71073 Å
d (g cm⁻³)	1.31
μ (mm⁻¹)	1.22
F(000)	1246
Crystal size (mm)	0.32×0.25×0.08
Data collection	
T_{min}, T_{max}	0.692, 1
h, k, l max	13, 14, 27
No. of measured, independent and observed [$I > 2\sigma(I)$] reflections	19849, 11395, 9664
θ_{min}, θ_{max} (°)	2.2, 28.7
R_{int}	0.047
$(\sin\theta/\lambda)_{max}$ (Å⁻¹)	0.606
Refinement	
$R[F^2 > 2\sigma(F^2)]$, $wR(F^2)$, S	0.055, 0.151, 1.07
No. of reflections	11,395
No. of parameters	731
No. of restraints	1
H-atom treatment	H-atom parameters constrained
$\Delta\rangle_{max}$, $\Delta\rangle_{min}$ (e Å⁻³)	1.49, −0.77
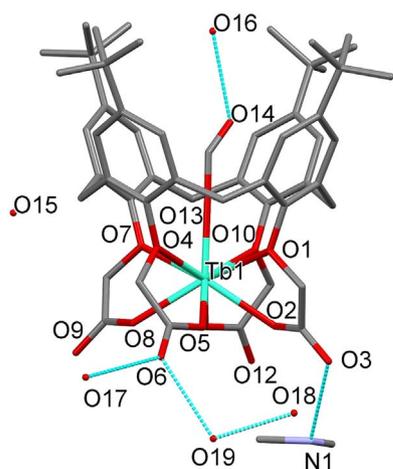
Fig. 1. Atom labeling in calix-TA-SC-Tb; all hydrogen atoms, and less populated disordered parts are omitted. Color code: light green – terbium, gray-carbon, red-oxygen, blue-nitrogen. Light blue dashed lines present intermolecular hydrogen bonds. (For interpretation of the references to color in this figure legend, the reader is referred to the web version of this article.)

than any network period). Because the formate anion is present inside the calix, the phenyl rings adopt the *cone* conformation with almost uniform mutual rings inclination; dihedral angles are 44.95° between C1-C6 and C27-C32 and 48.57° between C14-C19 and C40-C45. Molecules in the solid-state form flat 2D layers perpendicular to the **c** axis (Fig. 2). Each layer is hydrophobic outside due to the presence of *t*-butyl calixarene groups, and hydrophilic inside where (at z=0) ammonium and $H_5O_2^+$ cations together with water molecules are present, forming region strongly reinforced by a network of hydrogen bonding of O—H ...O and N—H ...O types. The layer can be viewed as a parallel assembly of dimers composed of two calixarene-formate-Tb
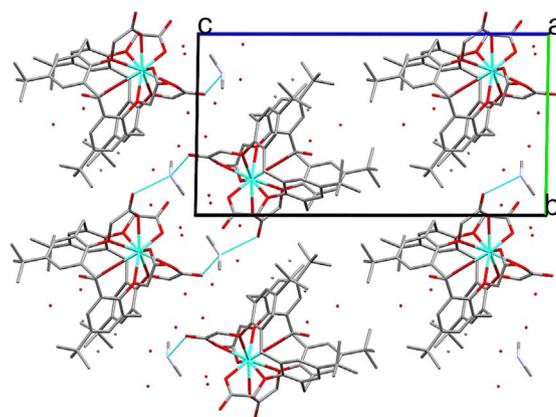
Fig. 2. Packing of calix-TA-SC-Tb viewed along the **a** axis. Hydrogen atoms omitted. Light blue dashed lines indicate NH...O hydrogen bonds. (For interpretation of the references to color in this figure legend, the reader is referred to the web version of this article.)

complexes linked by dimethylammonium-based hydrogen bonding.

Calix-TA-SC-Tb is the first example of the solid-state inclusion metal complex based on calix[4]arene-tetracarboxylate. A few examples of different *p-tert*-butyl-calix[4]arene derivatives with metal cations, including Eu³⁺ and Tb³⁺ have been reported [25,26]. Sabbatini et al. have revealed the preparation of the inclusion complex of *p-tert*-butyl-calix[4]arene tetra-diethylamide and Eu³⁺ [27]. As for the Tb-complex reported here, the Eu³⁺cation was coordinated by four ethereal and four carbonyl oxygen atoms.

3.3. Powder X-ray diffraction and IR spectra

The X-ray diffraction patterns of the samples calix-TA-Eu, calix-TA-Tb and calix-TA-Gd were compared with the XRD pattern of the pure ligand calix-TA and with the simulated pattern from the single-crystal structure of calix-TA-SC-Tb (Fig. 3). No peaks corresponding to the pure ligand were observed in the XRD pattern of the prepared samples indicating the formation of new structures. Although it was impossible to identify the obtained phases, it can be clearly seen, that the X-ray diffraction pattern of the complex is quite different from that obtained for samples calix-TA-Ln (Ln = Eu, Tb or Gd). This difference may suggest the formation of novel hybrid materials. The patterns of three calix-TA-Ln are very similar to each other; hence, it can be assumed that the prepared samples are isostructural.

The IR spectra of the obtained hybrid materials calix-TA-Eu, calix-TA-Tb, calix-TA-Gd and in comparison, of the pure ligand, are shown in Fig. 4. The strong band at 1746 cm⁻¹, observed in the pure ligand
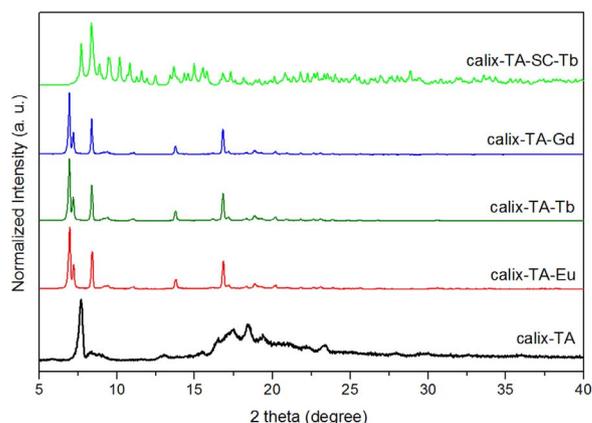
Fig. 3. PXRD patterns of the synthesized calix-TA-Ln samples (Ln = Eu, Tb, Gd) and of the pure ligand calix-TA, in comparison with the simulated from single-crystal data PXRD patterns of calix-TA-SC-Tb.
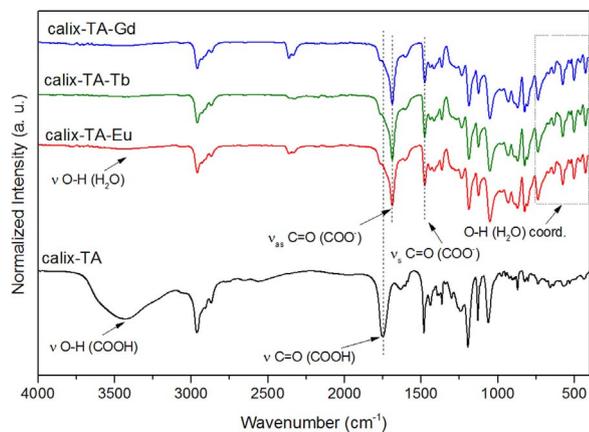
Fig. 4. FT-IR spectra of the pure ligand calix-TA <u>and</u> the hybrid materials calix-TA-Ln (Ln = Eu, Tb, Gd).

spectrum, corresponds to the stretching vibration ν (C=O) of the COOH groups. The residual band at around 1765 cm^{-1} in the spectra of calix-TA-Ln could be assigned to the protonated carboxylic acid groups with no hydrogen bonds between them. In such case, the band shift towards higher wavenumber is normally observed.

On the other hand, the presence of the strong band at 1688 cm^{-1} related to the stretching asymmetric vibrations of deprotonated carboxylates, suggests the formation of lanthanide-coordinated hybrids. We assume that one of the carboxylic acid groups remains protonated (as seen in IR spectra), whereas the other three groups are deprotonated and coordinated to the metal center. Although the IR spectra did not furnish irrefutable evidence on the hybrid structure, the difference between wavenumbers ($\Delta\nu$) of the stretching, asymmetric and symmetric vibrations of COO$^-$ groups provided useful information about coordination modes of carboxylate groups in the structure. The value of $\Delta\nu=208$ cm^{-1} indicates the presence of monodentate coordination modes, and most probably excludes the possibility of the chelate formation (as in the case of a single complex or a sandwich-type complex), for which the typical values of $\Delta\nu$ are much lower than 200 cm^{-1} [28]. Therefore, it is thought that the extended coordination hybrids were successfully synthesized. Further evidence should be furnished; therefore, some attempts to produce high-quality crystals of calix-TA-Ln will be performed. Noteworthy is the fact that single or sandwich-like complexes are typically soluble in some organic solvents, whereas the prepared samples calix-TA-Ln could not be dissolved in any organic solvent what may also indicate the formation of a polymer structure.

The broadband at around 3450 cm^{-1} can correspond to a water molecule present in the structure. The IR spectra of all samples also show bands in the region of 630–740 cm^{-1} and 500–620 cm^{-1} which may be ascribed to the presence of coordinated water molecules.

3.4. Photoluminescent properties

The luminescent properties of the hybrid materials calix-TA-SC-Tb, calix-TA-Tb and calix-TA-Eu were studied in the solid state at 298 K. The excitation and emission spectra of the sample calix-TA-Gd were recorded at 10 K.

The photophysical properties of two different Tb-hybrid materials, calix-TA-SC-Tb and calix-TA-Tb, were compared. The excitation and emission spectra profiles for both Tb-hybrids differ significantly (Fig. 5).

For calix-TA-SC-Tb, the excitation spectrum ($\lambda_{em}=544$ nm) shows two bands in the region of 250–330 nm centered at 289 and 320 nm, which correspond mostly to the $\pi \rightarrow \pi^*$ transitions of the calixarene ligand. However, terbium also has an accessible 5d-4f transition; thus inter-configurational 5d-4f transitions of Tb^{3+} ion may also be ob-

served in this region [29]. The intensity of bands in the region of 340–500 nm attributed to the typical *f-f* transitions of Tb^{3+} ion $^7F_6\rightarrow^5G_{J,}$ $^5D_2$, $^5D_3$, $^5D_4$, is much lower compared to the band attributed to $\pi\rightarrow\pi^*$ transitions. This fact indicates the occurrence of an energy transfer from the excited ligand level to the emitting state of Tb^{3+} ion (antenna effect) [30].

The excitation spectrum of calix-TA-Tb ($\lambda_{em}=544$ nm) presents a broadband in the whole spectral range corresponding to the $\pi \rightarrow \pi^*$ and/or 5d-4f transitions, which most probably overlaps the *f-f* transitions of Tb^{3+}.

The spectral emission profile for calix-TA-SC-Tb ($\lambda_{ex}=285$ nm) clearly shows the sharp peaks corresponding to the $^5D_4\rightarrow^7F_J$ (J=0,1, 2, 3, 4, 5 e 6) transitions of Tb^{3+} ion, with the most intense peak at 544 nm, which confers the intense green luminescence to the single Tb-complex. In the emission spectra of calix-TA-Tb ($\lambda_{ex}=289$ nm), bands attributed to the $^5D_4\rightarrow^7F_{6,5,4,3}$ transitions overlap the ligand-centered emission bands, what suggests that Tb^{3+} ion might not be efficiently sensitized by the coordination to the calixarene ligand in this system.

The emission spectra for calix-TA-Tb were also collected upon different excitation wavelengths equal to 313, 353 and 370 nm (Fig. S1). All spectra present a broad emission band of the ligand that overlaps Tb^{3+} emissions. The intensity of Tb^{3+} emissions was found to be dependent on the excitation wavelength and was the highest at $\lambda_{ex}=289$ nm.
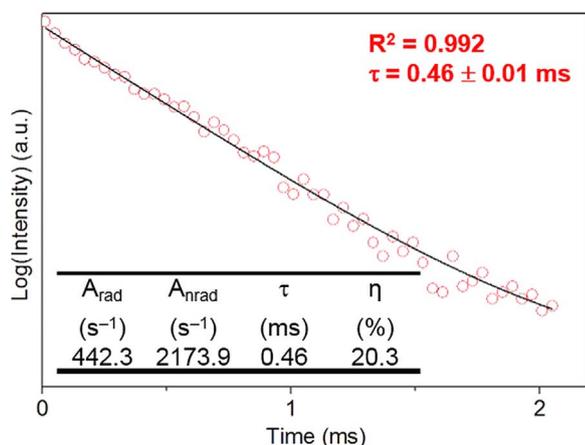
Comparing emission spectra of both Tb-hybrids, one can conclude that in the single complex calix-TA-SC-Tb, the energy transfer from the ligand to Tb^{3+} excited levels is probably more efficient than in the calix-TA-Tb. The favorable antenna effect observed in the case of calix-TA-SC-Tb might be due to the tight Tb^{3+} encapsulation by four calixarene carboxylate arms in the single complex. In the case of calix-TA-Tb, the possibility of the single-complex formation may be rather excluded (based on the XRD and IR data analysis). Thus, somehow, the packing of the calixarene unit and/or the coordination mode of carboxylates in the calix-TA-Tb hybrid might provide longer distances between the sensitizer and the lanthanide ion compared to the single complex, what consequently may lead to the less efficient energy transfer [30]. This is consistent with the IR spectra results which indicated monodentate coordination modes of carboxylates in the structure, what often leads to longer ligand-lanthanide distances.

The luminescence decay lifetimes for both Tb-samples were measured monitoring the $^5D_4$ emitting state (Fig. 6). The higher value of luminescence decay lifetime $\tau=1.63 \pm 0.01$ ms was found for calix-TA-SC-Tb, compared to $\tau=1.11 \pm 0.01$ ms obtained for calix-TA-Tb. The drop in the decay lifetime for calix-TA-Tb might be caused by the presence of water molecules in the inner coordination sphere of Tb^{3+} ion, what was not the case of calix-TA-SC-Tb. It is well established that the presence of water molecules in the lanthanide primary coordination sphere contributes to nonradiative de-excitation and a reduced luminescence lifetime.

Both curves were fitted to a monoexponential function suggesting that, in both hybrids, only one type of a coordination environment of Tb^{3+} is present.

The lifetime of calix-TA-SC-Tb is longer than those obtained (in solution) for some Tb-chelates based on polyaminocarboxylates (regarded as one of the most efficient chelators for lanthanides) reported by Li and Selvin [31]. For example, the Tb-chelate based on the linear diethylenetriaminepentaacetic acid (DTPA) or macrocyclic DOTA (1,4,7,10-tetraazacyclododecane-1,4,7,10-tetraacetic acid) have shown the luminescent decay lifetimes equal to 1.55 and 1.54 ms, respectively. In those cases, 1.1 water molecule was found to be coordinated in the inner sphere of lanthanide site. On the other hand, for triethylene-triaminehexaacetic acid (TTHA) and TETA (1,4,8,11-tetraazacyclote-tradecane-1,4,8,11-tetraacetic acid) polyaminocarboxylate chelates, the respective lifetimes were high (2.10 and 2.05), what was explained by the smaller water molecule number (0.22) present in the first coordination sphere of Tb^{3+} [31].

Fig. 5. Excitation (black line; λ_{em}=544 nm) and emission (green line; λ_{ex}=285 or 289 nm) spectra for (a) calix-TA-SC-Tb and (b) calix-TA-Tb in the solid state at room temperature. (For interpretation of the references to color in this figure legend, the reader is referred to the web version of this article.)

For calix-TA-Eu, the excitation spectrum (λ_{em}=615 nm; black line; Fig. 7) presents the bands in the region of 350–550 nm and 280–380 nm assigned to the characteristic *f-f* Eu^{3+} transitions from $^7F_{1,0}$ to $^5D_{1,2,4}$, $^5L_6$, ^5G_J states and to the ligand $\pi\rightarrow\pi^*$ transition, respectively. The emission spectra were collected upon two different excitation wavelengths (λ_{ex}=322 nm, dashed red line and λ_{ex}=393 nm, solid red line). Both emission spectra show a broadband between 400 and 600 nm attributed to the ligand emission. Also, sharp peaks corresponding to the europium $^5D_0\rightarrow^7F_J$ (J=0, 1, 2, 3, 4) transitions can be observed, with the most intense peak at 615 nm responsible for red luminescence of the hybrid. However, the excitation in the ligand level at 322 nm led to the more intense emission bands of Eu^{3+} when compared to the emission lines upon direct excitation in the Eu^{3+} level ($F_{1,0}\rightarrow^5L_6$). In the latter case, the ligand emission was predominant.

Since both hybrids calix-TA-Eu and calix-TA-Tb are isostructural (based on XRD and IR results), the relatively weak antenna effect observed for calix-TA-Eu (as for calix-TA-Tb), might be also related to the packing of the calixarene unit and/or the coordination mode of carboxylates in the solid.

The presence of the band attributed to the strongly forbidden electric dipole $^5D_0\rightarrow^7F_0$ transition in the spectrum (see Fig. S2), indicates a low symmetry environment around Eu^{3+} ions, typically C_{nv}, C_s, C_n. Furthermore, the ratio of the emission intensities between transitions $^5D_0\rightarrow^7F_2$ and $^5D_0\rightarrow^7F_1$, so-called asymmetry factor ($R_{02/01} = \frac{^5D_0 \rightarrow \, ^7F_2}{^5D_0 \rightarrow \, ^7F_1}$), gives more information about the degree of environment asymmetry around Eu^{3+} ion [32]. A high ratio equal to 5.22 confirms a low-symmetry coordination site of Eu^{3+} in calix-TA-Eu. This value is much greater than for a typical calixarene-Eu^{3+} inclusion complex reported in the literature ($R_{02/01}$=2.73) [32]. The careful analysis of the splitting of each Eu^{3+} transitions may suggest that the Eu^{3+} is embed in

Fig. 7. Excitation (black line, λ_{em}=615 nm) and emission (dashed red line, λ_{ex}=322 or solid red line, λ_{ex}=393 nm) spectra of calix-TA-Eu obtained in the solid state at room temperature. (For interpretation of the references to color in this figure legend, the reader is referred to the web version of this article.)

the C_3 symmetry-site, according to the diagram elaborated by Sengupta et al. [32].

The luminescence decay curve for calix-TA-Eu (Fig. 8) was fitted with a monoexponential function, indicating only one symmetry site around Eu^{3+} ion. This result may support our assumption that both hybrids calix-TA-Tb and calix-TA-Eu are isostructural, both having only one lanthanide coordination site.

The inset table in Fig. 8 summarizes the experimental values for the radiative (A_{rad}) and non–radiative (A_{nrad}) rates of the spontaneous Eu^{3+} emission, as well as the emission quantum efficiency (η). The hybrid calix-TA-Eu exhibits relatively short luminescence lifetime

Fig. 6. Luminescence decay curve for (a) calix-TA-SC-Tb and (b) calix-TA-Tb monitoring emission at λ=544 nm.

Fig. 8. Luminescence decay curve for calix-TA-Eu (λ_{ex}=322 nm, λ_{em}=615 nm) and luminescence parameters (inset table).
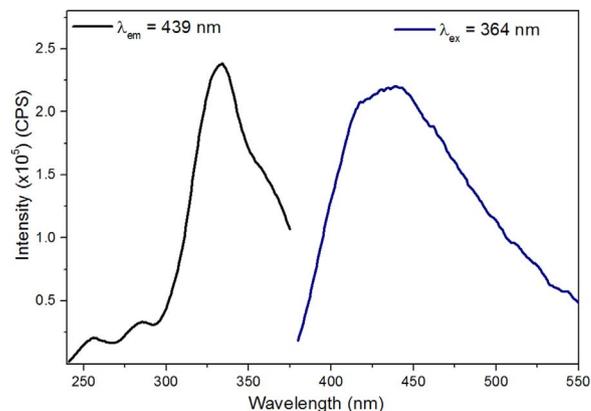

Fig. 9. Excitation (black line; λ_{em}=450 nm) and emission spectra (blue line; λ_{ex}=328 nm) obtained for calix-TA-Gd in the solid state at 10 K. (For interpretation of the references to color in this figure legend, the reader is referred to the web version of this article.)

Fig. 10. Proposed energy level diagram for calix-TA-Eu, calix-TA-Tb and calix-TA-Gd, showing possible processes of an intramolecular energy transfer.

(τ=0.46 ms) and a high contribution of non–radiative decays, deactivating the system (A_{nrad}=2173.9 s^{-1}). However, the obtained value of emission quantum efficiency equal to 20.3% is greater than that reported for other calixarene-based systems [22].

The lifetime obtained for calix-TA-Eu (τ=0.46) is lower than for the corresponding calix-TA-Tb hybrid (τ=1.11) reported here. Such difference was rather expected as Tb^{3+} ion is less sensitive, compared to Eu^{3+}, to non-radiative deactivation caused mainly by water molecules attached to the Ln^{3+} center. Moreover, the significant energy gap between Tb^{3+} excited states and the lower energy states from ^7F term is advantageous for a Tb^{3+} emission, whereas Eu^{3+} excited state may undergo non-radiative deactivation easily due to the close-situated excitation energy levels. As a result, the luminescence of terbium is, providing appropriate energy levels of the ligand, in general, more efficient than the luminescence of europium and longer lifetimes are commonly observed [29].

Rudkevich et al. have reported a series of Tb-complex of calix[4] arene based on three carboxylic acid groups which showed lifetimes measured in MeOH in the range of 0.55–0.65 ms. Similar decay lifetimes the authors have found for the analogous Eu-complexes (0.60–0.65 ms) [33]. For the tetraacetamide derivative of calix[4] arene, the lifetimes measured in MeOH solution were τ=1.5 and 0.65 ms, for Tb^{3+} and Eu^{3+} complexes, respectively [34]. It is well known, however, that the luminescent properties measured in solution and the solid-state may differ significantly [27]. The lifetime of the solid-state Eu-complex based on tetraacetamide derivative of calix[4] arene (measurements at liquid helium temperature) was found to be biexponential with τ_1=0.5 ms and τ_2=1.3 ms [27]. Therefore, the comparison of our results with those obtained previously is rather difficult.

Because Gd^{3+} is a nonemissive ion, it may be used to investigate energy levels of the coordinated ligand by the measurements of the phosphorescence spectrum of the gadolinium analog structure [29]. Since compounds containing Gd^{3+} typically do not exhibit luminescence in the visible region when excited by ultraviolet radiation, the observed luminescence processes for calix-TA-Gd can be exclusively associated with the coordinated ligand.

The excitation spectrum of calix-TA-Gd (Fig. 9; black line) obtained by monitoring λ_{em}=450 nm presents four bands in the range of 240–375 nm, corresponding to the $\pi \rightarrow \pi^*$ transitions in the aromatic groups of the calixarene. The emission spectra with λ_{ex}=328 nm (Fig. 9; blue line) show the broadband centered at 450 nm. It has been reported that the free calixarene-based ligand shows an absorption spectrum in the range of 250–350 nm and the emission spectrum in the range of 420–550 nm with the maximum at 455 nm [35]. Therefore, our results are consistent with the literature data. In our case, the blue shift of the
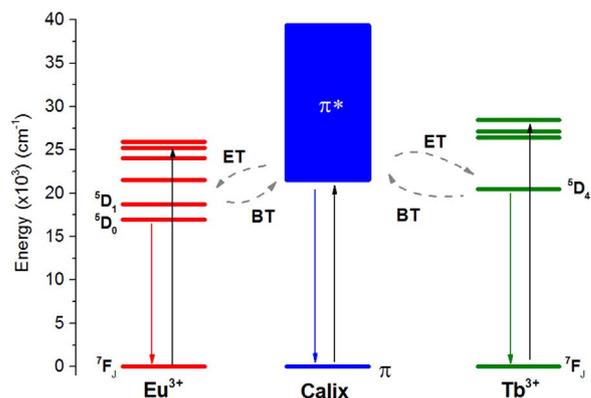
maximum emission band from 455 to 450 nm may be caused by the coordination of the ligand to the Gd^{3+} center.

On the basis of the emission and excitation spectra, the proposed energy diagrams for hybrids calix-TA-Eu, calix-TA-Tb and calix-TA-Gd, were constructed (Fig. 10). It is well known that for the efficient sensitization of Eu^{3+} and Tb^{3+}, the energy levels of a ligand should be located above $^5D_0$ (> 17 500 cm^{-1}) and $^5D_4$ (> 20 200 cm^{-1}) excited levels of Eu^{3+} and Tb^{3+}, respectively [29]. For calix-TA-Eu and calix-TA-Tb, the excited π^* levels of the ligand (21 470 cm^{-1}) lie above and close to the emitting $^5D_0$ (Eu^{3+}) and $^5D_4$ (Tb^{3+}) excited levels, what enhances the antenna effect.

On the other hand, the presence of the intense band ($\pi^* \rightarrow \pi$ transitions) in the emission spectra observed for calix-TA-Eu and calix-TA-Tb may be explained by the possible energy back-transfer mechanism (BT) from the lanthanide levels to the ligand excited levels.

It has been established that the optimal ligand levels should be located just above the $^5D_2$ (22,000 cm^{-1}) Eu^{3+} excited state to avoid the energy back transfer process [28]. In our case, the lowest excited π^* level is situated slightly below this value, at around 21,470 cm^{-1}, what may enhance BT process.

In the case of calix-TA-Eu, the energy transfer may also occur from the ligand excited state to the higher-energy excited states of Eu^{3+}, followed by non-radiative deactivation to the $^5D_0$ emitting state. Therefore, the luminescence decay lifetimes for calix-TA-Eu are expected to be shorter than for the corresponding calix-TA-Tb, what was indeed observed. The presence of water molecules coordinated to the Eu^{3+} center may also contribute to the non-radiative deactivation of the Eu^{3+} excited states and quench the luminescence.

4. Conclusions

The reaction between Ln chlorides (Ln = Eu, Tb or Gd) and *p-tert*-butylcalix[4]arene-tetracarboxylic acid (calix-TA) in the 1:3 M ratio, performed in a DMF/ACN at 90 °C for 4 days, provided three isostructural lanthanide hybrid materials calix-TA-Ln. The results of PXRD and IR indicated the formation of extended coordination compounds with monodentate coordination modes of carboxylates. When the synthesis was repeated using 1:1 M ratio and shorter time of reaction (1 day), crystals of the single complex calix-TA-SC-Tb were obtained. Both Tb-hybrids showed antenna effect but longer luminescence decay lifetime was observed for calix-TA-SC-Tb what may be ascribed to the tight encapsulation of Tb^{3+} ion in the single complex. Calix-TA-Tb and calix-TA-Eu exhibited the monoexponential luminescence decay lifetime indicating only one type of coordination environment of the lanthanide ion (Tb or Eu). The analysis of emission peaks in the spectrum of calix-TA-Eu suggested that Eu^{3+} occupy a low-symmetry site in the structure, estimated as C_3. The investigation of the energy levels of calixarene-ligand in calix-TA-Ln systems demonstrated that the possible energy-back transfer might occur, supported by the observation of the ligand-centered emission in the spectra of calix-TA-Tb and calix-TA-Eu. Our results showed that Eu^{3+} and Tb^{3+} can be sensitized by the calix[4]arene-tetracarboxylate ligand and the energy back-transfer process depends on the packing and the orientation of the calixarene-ligand in a structure. Further work on these and new calixarene-based luminescent frameworks is needed to investigate the structure-property relationship in details.

Supporting information

X-ray crystallographic information file (CIF) of calix-TA-SC-Tb is available free of charge via the Internet from the Cambridge Crystallographic Data Center (CCDC) upon request (http://www.ccdc.cam.ac.uk, CCDC deposition number 1510908 or via the Internet at http://www.sciencedirect.com. Details on the crystal structure refinement for calix-TA-SC-Tb and additional figures related to luminescent properties are revealed in the Supporting Information and are available free of charge via the Internet at http://www.sciencedirect.com.

Acknowledgements

Appendix A. Supplementary material

Supplementary data associated with this article can be found in the online version at doi:10.1016/j.jssc.2017.04.002.

References

[1] J. Vicens, V. Bohmer, Calixarenes: A Versatile Class of Macrocyclic Compounds, Springer, Netherlands, 1991.

[2] J. Vicens, J. Harrowfield, Calixarenes in the Nanoworld, Springer, 2007.

[3] W. Sliwa, T. Girek, Calixarene complexes with metal ions, J. Incl. Phenom. Macrocycl. Chem. 66 (2010) 15–41.

[4] H. Zhang, R. Zoub, Y. Zhao, Macrocycle-based metal-organic frameworks, Coord. Chem. Rev. 292 (2015) 74–90.

[5] K. Xiong, M. Wu, Q. Zhang, W. Wei, M. Yang, F. Jiang, M. Hong, 1D Infinite silver(I) chains reside in the big cavities built by the novel *p*-sulfonatocalix[4]arene-trisilver blocks, Chem. Commun. 14 (2009) 1840–1842.

[6] C. Chen, J.-F. Ma, B. Liu, J. Yang, Y.-Y. Liu, Two unusual 3D copper(II) coordination polymers constructed by *p*-sulfonated calixarenes and Bis(triazolyl) ligands, Cryst. Growth Des. 11 (2011) 4491–4497.

[7] Y. Liu, W. Liao, Y. Bi, X. Wang, H. Zhang, Assembly of seven supramolecular compounds with p-Sulfonatocalix[6]arene, Cryst. Growth Des. 9 (2009) 5311–5318.

[8] S.P. Bew, A.D. Burrows, T. Duren, M.F. Mahon, P.Z. Moghadam, V.M. Sebestyen, S. Thurston, Calix[4]arene-based metal–organic frameworks: towards hierarchically porous materials, Chem. Commun. 48 (2012) 4824–4826.

[9] L.-L. Liu, Z.-G. Ren, L.-W. Zhu, H.-F. Wang, W.-Y. Yan, J.-P. Lang, Temperature-driven assembly of Ln(III) (Ln = Nd, Eu, Yb) coordination polymers of a flexible azo calix[4]arene polycarboxylate ligand, Cryst. Growth Des. 11 (2011) 3479–3488.

[10] C. Redshaw, O. Rowe, D.L. Hughes, A.-M. Fuller, I.A. Ibarra, S.M. Humphrey, New structural motifs in lithium and zinc calix[4]arene chemistry, Dalton Trans. 42 (2013) 1983–1986.

[11] Y.-Y. Liu, C. Chen, J.-F. Ma, J. Yang, A series of complexes constructed by different calix[4]arene derivatives, CrystEngComm 14 (2012) 6201–6214.

[12] N. Sabbatini, M. Guardigli, A. Mecati, V. Balzani, R. Ungaro, E. Ghidini, A. Casnati, A. Pochini, Encapsulation of lanthanide ions in calixarene receptors. A strongly luminescent terbium (3+) complex, J. Chem. Soc. Chem. Commun. (1990) 878–879.

[13] J.L. Atwood, L.J. Barbour, S. Dalgarno, C.L. Raston, H.R. Webb, Supramolecular assemblies of *p*-sulfonatocalix[4]arene with aquated trivalent lanthanide ions, J. Chem. Soc. Dalton Trans. 23 (2002) 4351–4356.

[14] F. Arnaud-Neu, G. Barret, S. Cremin, M. Deasy, G. Ferguson, S.J. Harris, A.J. Lough, L. Guerra, M.A. McKervey, M.J. Schwinghyphen, P. Weill, Schwinte, Selective alkali-metal cation complexation by chemically modified calixarenes. Part 4. Effect of substituent variation on the Na^+/K^+ selectivity in the ester series and X-ray crystal structure of the trifluoroethyl ester, J. Chem. Soc. Perkin Trans. 2 (1992) 1119–1125.

[15] F. Arnaud-Neu, E.M. Collins, M. Deasy, G. Ferguson, S.J. Harris, B. Kaitner, A.J. Lough, M.A. McKervey, E. Marques, Synthesis, X-ray crystal structures, and cation-binding properties of alkyl calixaryl esters and ketones, a new family of macrocyclic molecular receptors, J. Am. Chem. Soc. 111 (1989) 8681–8691.

[16] P.R.O. CrysAlis, Agilent Technologies, Version 1.171.35.15, Abingdon, England, 2011.

[17] L. Palatinus, G. Chapuis, *SUPERFLIP* – a computer program for the solution of crystal structures by charge flipping in arbitrary dimensions, J. Appl. Cryst. 40 (2007) 786–790.

[18] G.M. Sheldrick, A short history of *SHELX*, Acta Crystallogr. A 64 (2008) 112–122.

[19] L.J. Farrugia, *WinGX* suite for small-molecule single-crystal crystallography, J. Appl. Crystallogr. 32 (1999) 837–838.

[20] C.F. Macrae, I.J. Bruno, J.A. Chisholm, P.R. Edgington, P. McCabe, E. Pidcock, L. Rodriguez-Monge, R. Taylor, J. van de Streek, P.A. Wood, *Mercury CSD 2.0* – new features for the visualization and investigation of crystal structures, J. Appl. Crystallogr. 41 (2008) 466–470.

[21] K. Binnemans, Interpretation of europium(III) spectra, Coord. Chem. Rev. 295 (2015) 1–45.

[22] X.-F. Qiao, H.-Y. Zhang, B. Yan, Dalton Trans. Photoactive Binary and Ternary Lanthanide (Eu^{3+}, Tb^{3+}, Nd^{3+}) Hybrids with *p-tert*-butylcalix[4]arene Derived Si–O Linkages and Polymers, vol. 39, 2010, pp. 8882–8892.

[23] N. Toropava, I. Persson, L. Eriksson, D. Lundberg, Hydration and hydrolysis of thorium(IV) in aqueous solution and the structures of two crystalline thorium(IV) hydrates, Inorg. Chem. 48 (2009) 11712–11723.

[24] B. Leśniewska, O. Danylyuk, K. Suwinska, T. Wojciechowski, A.W. Coleman, Supramolecular versatility in the solid-state complexes of para-sulfonatocalix[4]arene with phenanthroline, Cryst. Eng. Comm. 13 (2011) 3265–3272.

[25] D. D'Alessio, S. Muzzioli, B.W. Skelton, S. Stagni, M. Massi, M.I. Ogden, Luminescent lanthanoid complexes of a tetrazole-functionalised calix[4]arene, Dalton Trans. 41 (2012) 4736–4739.

[26] Luminescent probes by N. Sabbatini, M. Guardigli, I. Manet, R. Ziessel, in Calixarenes, Ed Z. Asfari et al, 2001 Kluwer Academic Publishers, Netherlands, 2001, pp. 583–597.

[27] M.F. Hazenkamp, G. Blasse, N. Sabbatini, R. Ungaro, The solid state luminescence of the encapsulation complex of Eu^{3+} in *p-t*-Butyl-calix[4]arene tetraamide, Inorg. Chim. Acta 172 (1990) 93–95.

[28] G.B. Deacon, R.J. Phillips, Relationships between the carbon-oxygen stretching frequencies of carboxylate complexes and the type of carboxylate coordination, Coord. Chem. Rev. 33 (1980) 227–250.

[29] J. Andresand, A.-S. Chauvin, The rare earth elements. Fundamentals and Applications, in: D.A. Atwood (Ed.)Chapter: Lanthanides: Luminescence Applications, John Wiley & Sons Ltd., 2012, pp. 135–152.

[30] G.F. de Sá, O.L. Malta, C.M. Donegá, A.M. Simas, R.L. Longo, P.A. Santa-Cruz, E.F. da Silva Jr., Spectroscopic properties and design of highly luminescent lanthanide coordination complexes, Coord. Chem. Rev. 196 (2000) 165–195.

[31] M. Li, P.R. Selvin, Luminescent polyaminocarboxylate chelates of terbium and europium: the effect of chelate structure, J. Am. Chem. Soc. 117 (1995) 8132–8138.

[32] A. Sengupta, S.V. Godbole, P.K. Mohapatra, M. Iqbal, J. Huskens, W. Verboom, Judd–Ofelt parameters of diglycolamide-functionalized calix[4]arene Eu^{3+} complexes in room temperature ionic liquid for structural analysis: effects of solvents and ligand stereochemistry, J. Lumin. 148 (2014) 174–180.

[33] D.M. Rudkevich, W. Verboom, E. van der Tol, C.J. van Staveren, F.M. Kaspersen, J.W. Verhoeven, D.N. Reinhoudt, Calix[4]arene-triacids as receptors for lanthanides; synthesis and luminescence of neutral Eu^{3+} and Tb^{3+} complexes, J. Chem. Soc. Perkin Trans. 2 (1995) 131–134.

[34] N. Sabbatini, M. Guardigli, A. Mecati, V. Balzani, R. Ungaro, E. Ghidini, A. Casnati, A. Pochini, Encapsulation of lanthanide ions in calixarene receptors. A strongly luminescent terbium (3+) complex, J. Chem. Soc. Chem. Commun. (1990) 878–879.

[35] S.V. Shevchuk, E.A. Alexeeva, N.V. Rusakova, Y.V. Korovin, V.A. Bacherikov, A.I. Gren, Some new properties of calixarenes: the luminescence of four lanthanide ions in calixarene complexes, Mendeleev Commun. 8 (1998) 112–113.